

Effects of Mg Content on Zn_{1-x}Mg_xO:Al Transparent Conducting Films

Xiaonan Li, Hannah Ray, Craig L. Perkins, and Rommel Noufi
5200, NREL, 1617 Cole Blvd., Golden, CO, 80401

ABSTRACT

Conductive zinc oxide (ZnO) films are used extensively as transparent electrodes in thin-film photovoltaic solar cells. Compared with the widely used indium tin oxide (ITO) and tin oxide (SnO₂), ZnO has a smaller optical bandgap. ZnO is commonly used as a front contact for copper indium gallium diselenide (CIGS) solar cells, but it forms a small, unfavorable conduction-band offset with the CdS layer. The optical bandgap of ZnO could easily be engineering by alloying with MgO or CdO. In this work, we try to optimize the ZnO for CIGS solar cells. The optical and electrical properties of Zn_{1-x}Mg_xO:Al films fabricated by co-sputtering were studied. Two targets: ZnO:Al and MgO, were used. The ratio of ZnO/MgO was varied continuously on the 6" x 6" glass substrate, and the effects of composition on the properties of the Zn_{1-x}Mg_xO:Al films were investigated. The carrier concentration and mobility of the Zn_{1-x}Mg_xO:Al films decreased quickly with increasing Mg content. However, the optical properties of the Zn_{1-x}Mg_xO:Al films do not vary linearly with Mg content, as reported by most papers. The observed optical bandgap of Zn_{1-x}Mg_xO:Al films is actually first narrowed, then increased with the Mg content. The shift in optical bandgap from narrow to wide occurs at around a composition of x = 0.07. After the point of x = 0.07, the bandgap width start increase but film sheet resistance already too low. Our result therefore suggests that the alloyed Zn_{1-x}Mg_xO:Al does not benefit the CIGS solar cell.

INTRODUCTION

The energy conversion efficiencies for thin-film photovoltaics such as multijunction amorphous silicon (a-Si), copper indium gallium diselenide (CIGS), and cadmium telluride (CdTe) solar cells have reached the point such that any improvement of the top window layer would significantly enhance the efficiency values. The goal of this study of the ZnO transparent conducting oxide (TCO) window layer is to optimize its properties for CIGS solar cells. ZnO is used as a front-contact layer for CIGS solar cells because of its high optical transmittance and low fabrication temperature. However, a conduction-band offset of -0.3 eV between ZnO and CdS reduces the cell open-circuit voltage (V_{oc}) [1]. On the other hand, if the ZnO bandgap can be widened, some current could still be gained in the short-wavelength range. Furthermore, if both the short-circuit current density (J_{sc}) and V_{oc} of the device are improved, then the fill factor (FF) will also be improved. Thus, widening the bandgap of ZnO by lifting the conduction band would improve the CIGS cell efficiency.

The band structure of ZnO can be engineering by alloying with MgO to form new compounds with appropriate optical and electronic properties. Studies have shown that bandgap engineering is possible for zinc magnesium oxide alloys, Zn_{1-x}Mg_xO (0 < x < 1). Choopun et al. and Matsubara et al. have done studies using pulsed-laser deposition and created Zn_{1-x}Mg_xO alloys with bandgaps above 5 eV [2,3], and Matsubara et al. created films with resistivities < 10⁻³ Ω-cm with bandgaps ranging from 3.5–3.97 eV and optical transmittance > 90% [3]. However, the above-mentioned studies are mainly on just a few separated x values. Our co-sputtering technique allows us to create a composition gradient to continuously vary the Mg content, x, of the film. A wide range of x from 0.03 to 0.33, along with deposition temperature variation, was studied, and the optical and electronic properties of the films were measured.

EXPERIMENTAL

$Zn_{1-x}Mg_xO:Al$ films are deposited by an AJA International ATC 2200-V RF magnetron sputtering system, which has the ability to co-sputter. The rotatable substrate station is positioned over the two targets that are tilted toward the substrate and positioned in line with each other, as shown in Fig. 1. The $ZnO:Al$ target is 99.999% pure with 98 wt% ZnO and 2 wt% Al_2O_3 (1.56 at% Al). The MgO target is 99.95% pure. The targets are purchased from Cerac Inc. and used as received. The substrate used is 6" x 6" 1737 Corning glass. The vacuum system base pressure is typically maintained at 2×10^{-8} torr, and the working pressure is chosen as 5×10^{-3} torr, with an argon gas flow of 40 sccm. The RF power is varied between 60 and 240 watts, depending on the desired Mg content and deposition rate. The thermocouple used for temperature control is about a centimeter from the substrate, so the substrate temperature could deviate somewhat from the controlled temperature. The temperature calibration uses a SensArray Corporation Thermocouple Instrumental Wafer. During the calibration, only the heater is powered on; the RF power is turned off. The calibrated temperature is used in this report. ZnO film thickness is determined using a Veeco Dektak 8 profilometer. A Cary 5G spectrophotometer is used to acquire the ultraviolet (UV)/visible/near-infrared (NIR) transmittance and reflectance spectra. The film electrical properties are measured using Hall effect equipment (BioRad model HL5500 system).

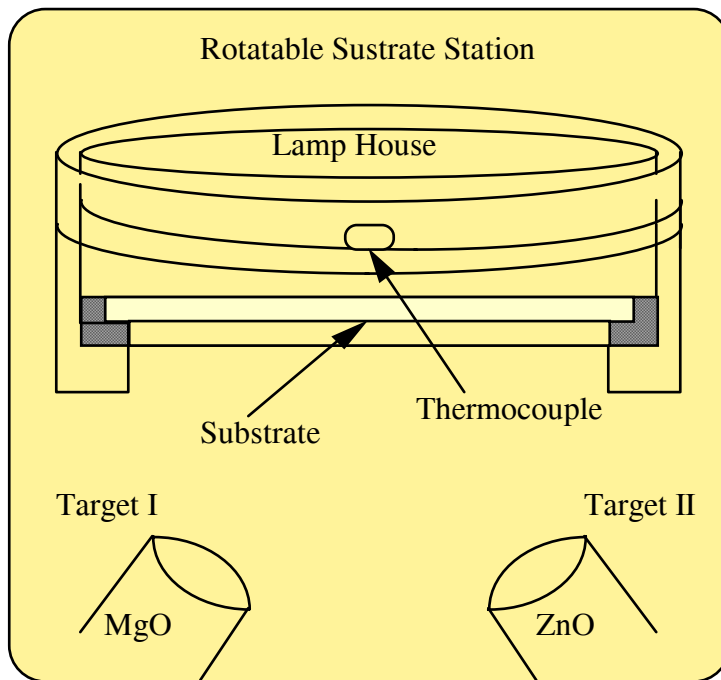


Figure 1. Schematic of RF magnetron sputtering system.

identify the relative position. All the characterizations for optical and electrical properties were performed at room temperature.

The spatial distribution of baseline deposition rates (DR) for each target $ZnO:Al$ or MgO was determined by using one sputtering gun at a time and not rotating the substrate station. These spatial distributions of DR are then used to estimate the $Zn:Mg$ ratios created later in the co-sputtering experiments. A co-sputter with both targets power-on was used to generate the combinatorial samples. Without rotating the substrate station, the composition gradient was created on the substrates. The Zn and Mg contents on the substrate depend on the relative position to the targets were estimated by previous obtained DR. The sputtering power was further adjusted to obtain a wide range of x values. Following deposition, the sample points were taken along the composition gradient and labeled to

RESULTS AND DISCUSSION

Using two sputtering guns (ZnO:Al and MgO), we generated four $Zn_{1-x}Mg_xO:Al$ film-coated libraries on 6" x 6" glass substrates. The content of the Mg, x , was calculated from the spatial distribution of the DR previously determined. X-ray photoelectron spectroscopy (XPS) was used to analyze several samples, and the results were compared with calculated x values. Figure 2 shows that the calculated values are in good agreement with measured values. Thus, all the x value data used in this study are calculated values. XPS also indicated that the oxygen content in the $Zn_{1-x}Mg_xO:Al$ are varied with x . As x increase, the oxygen-to-metal ratio increased.

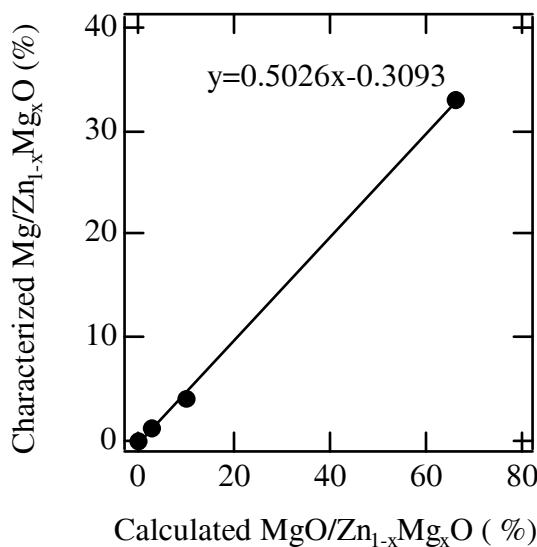


Figure 2. The XPS data indicates that the calculated MgO percentage is in good agreement with the actual number.

agreement with others.[5,6] We believe the observed variation of bandgap in region I is not due to bowing, but rather, to the interaction of Mg and Al dopant, as discussed in more detail below.

Figure 3 shows a plot of the bandgap, E_g , obtained from optical measurement, as a function of value x . In region II, the plot of E_g vs. x could be fit with a straight line: $y = 1.938x + 3.32$, which agrees well with the previous study [5]. The bandgap of a compound $A_{1-x}B_xC$ can be expressed as:

$$E_g(x) = (E_{BC} - E_{AC})x + E_{AC}. \quad (1)$$

Because the bandgap of pure ZnO is 3.32 eV, this fitting gives the bandgap of E_{BC} as 5.26 eV. However, the bandgap of MgO is about 7 eV. The obtained E_{BC} is much lower than this number. We know that the crystal structure of compound $Zn_{1-x}Mg_xO$ will change from hexagonal to cubic as x is varied from 0 to 1. Thus, there is no single fitting available for the whole region of $0 < x < 1$ and that can explain why the bandgap of MgO we obtained is lower

Optical and electrical measurements were taken every centimeter along the composition-gradient direction. The optical bandgap was calculated from the optical transmittance (T) and reflectance (R) spectra [4]. As the amount of Mg in the $Zn_{1-x}Mg_xO:Al$ alloy increased, the optical absorption edge shifted. However, it was not as reported previously by most papers, that it simply increased. The direction of the shift is different in two regions (Fig. 3, regions I and II), separated by the line where x is ~ 0.07 . In region I, the value of x is smaller than 0.07 and the optical absorption edge shifts to long wavelengths with increasing x , which indicates a decreased bandgap. This observation was not reported previously. In region II, the value of x is larger than 0.07, the absorption edge shifts to short wavelengths, which indicates an increase in bandgap. In this region, our observation is in good

than its actual value. In region I, the measured E_g actually continues to increase as x approaches zero, which is opposite of what most people observed.

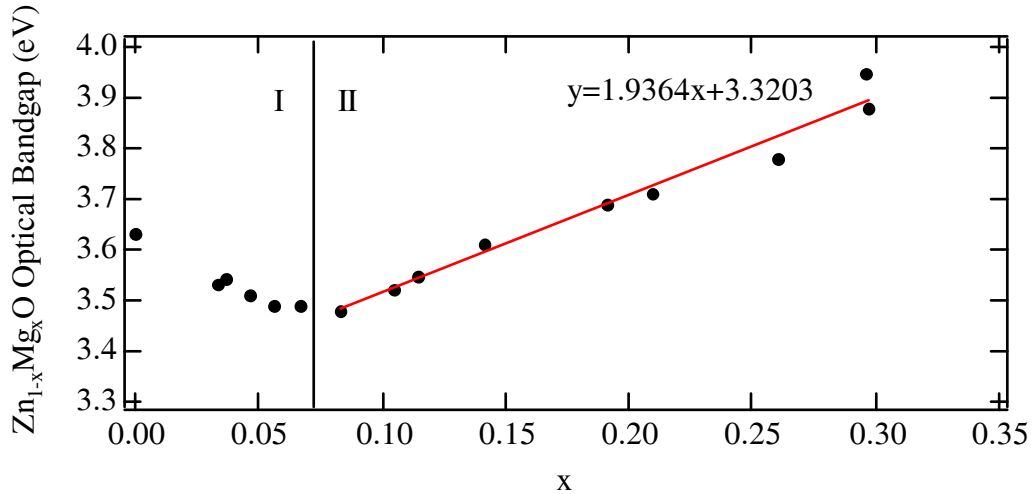


Figure 3. Observed optical bandgap vs. x , the proportion of Mg in the alloy, for a sample deposited at 100°C.

Figure 4 shows a plot of the electrical properties of the $\text{Zn}_{1-x}\text{Mg}_x\text{O}: \text{Al}$ film vs. x . As x increased, carrier mobility and carrier concentration both decreased, while resistance increased sharply. At values of $x > 0.035$ (3.5% MgO) in the alloy, the film resistivity was already one order of magnitude higher than that at $x = 0$. At values of $x > 0.08$, the sheet resistance became very high and the sign of the carrier concentration was positive. Because of the extremely low mobility, the positive reading could indicate large uncertainty. Thus, we stopped collecting Hall data at x equal to or greater than 0.08. Compare with Matsubara's work, the obtained carrier concentration decreases much quick as x increase. However, it fit with the optical data and can be explained well by the analysis conduct in the next paragraph.

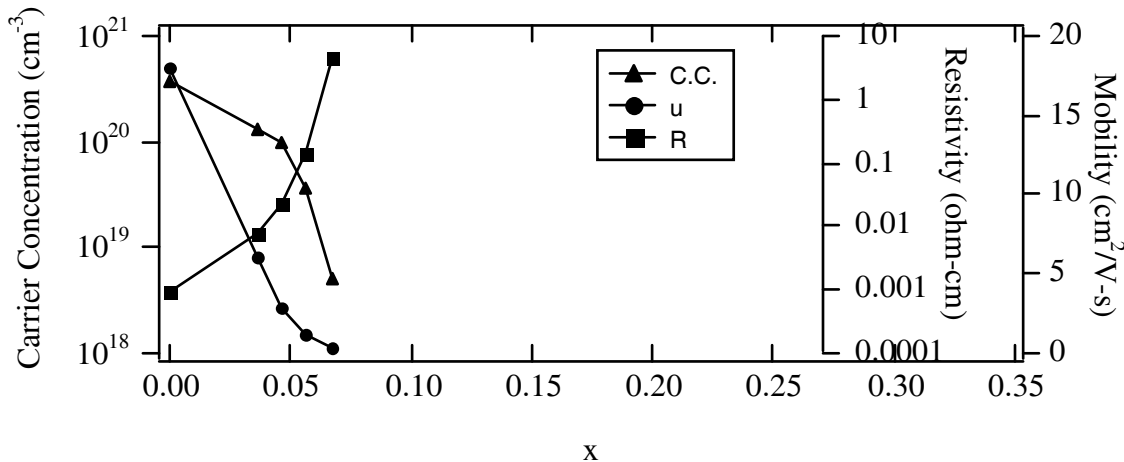


Figure 4. Electrical properties as a function of x . Data are taken from the same sample set as Fig. 3.

Combining the electrical data with optical data, we believe the observed optical bandgap narrowing with increased x in region I is caused by the following effects. First, at MgO content x equal to zero, ZnO is heavily doped by Al, and the optical bandgap of ZnO:Al will be affected by the doping. Under heavy doping conditions, the materials with small effective mass of electrons will clearly show the Burstein-Moss effect. The effective mass of electrons for ZnO is $0.24m_0$, at $T=300$ K, and the effective density of the conduction-band states (N_C) of ZnO is $6 \times 10^{18} \text{ cm}^{-3}$. [7,8] Thus, when the donor impurity density (N_D) equals $6 \times 10^{18} \text{ cm}^{-3}$, the Fermi level of ZnO moves into the conduction band and ZnO becomes degenerate. The observed optical bandgap E_O is therefore given by [9]:

$$E_O = E_g + \Delta E_{gBM} . \quad (2)$$

The ΔE_{gBM} due to the Burstein-Moss effect can be calculated by [10]:

$$\Delta E_{gBM} = \frac{4 \times 10^{-15}}{\frac{m_e^*}{m_0}} n^{\frac{2}{3}} \text{ eV} \quad (3)$$

Second, under heavy doping, bandgap narrowing (BGN) will be introduced, and the bandgap change, ΔE_{gBN} , can be expressed as [11]:

$$\Delta E_{gBN} = -\frac{a}{10^8} (n)^{\frac{1}{2}} + b \text{ meV} \quad (4)$$

where a and b are experimentally defined constants and n is carrier concentration. Third, the fundamental bandgap of $\text{Zn}_{1-x}\text{Mg}_x\text{O}$ will enlarge due to the alloy effect. Assuming that the equation, $y = 1.938x + 3.32$, obtained in region II is valid through x values smaller than 0.07. Thus, the observed optical bandgap E_O would be affected by above three factors and the sum can be expressed as:

$$E_O(\text{Zn}_{1-x}\text{Mg}_x\text{O}: \text{Al}) = E_g(\text{ZnO}: \text{Al}) + \Delta E_{gBN} + \Delta E_{gBM} + 1.938x . \quad (5)$$

By using value of carrier concentration obtained from Hall measurement, we can calculate the ΔE_{gBM} . From equation(5) we can get the estimated ΔE_{gBN} . Table 1 lists the different parts of ΔE_g 's as a function of x .

Table 1. ΔE values as a function of x .

x	E_O	ΔE_{gBN} (meV)	ΔE_{gBM} (meV)	$1.938x$ (meV)
0	3.63	-560	870	0
0.0362	3.54	-284	434	70
0.0469	3.51	-258	357	91
0.0564	3.49	-124	184	109
0.0668	3.48	-18.3	48.8	129

From this result, we can further calculate experimentally the constant a and b in Eq. (4). By plotting ΔE_{gBN} as a function of $(n)^{1/2}$, we get $a = 30$ and $b = 61.5$. Thus,

$$\Delta E_{gBN} = -\frac{30}{10^8} (n)^{\frac{1}{2}} + 61.5 \text{ meV} \quad (6)$$

Therefore, as the Mg content in $\text{Zn}_{1-x}\text{Mg}_x\text{O}: \text{Al}$ increases and the bandgap enlarge, the free carriers would decrease. Consequently, the quantities of $\Delta E_{gBN}(x)$ and $\Delta E_{gBM}(x)$ would decrease. Once the x value becomes larger than 0.07, carrier concentration becomes less than N_C ($6 \times 10^{18} \text{ cm}^{-3}$), and the ΔE_g values due to the doping effect can be ignored. The observed optical

bandgap, $E_o(Zn_{1-x}Mg_xO:Al) = E_g(ZnO:Al) + 1.938x$, that is what we find in region II. Our results indicate that if a higher conduction band were desired by the alloy method, then x would be over 0.15. At this x value, the film electrical property does not satisfy the requirement as a conductive window layer for the solar cell.

CONCLUSIONS

To optimize the properties of $Zn_{1-x}Mg_xO:Al$ alloy for CIGS solar cells, we formed $Zn_{1-x}Mg_xO:Al$ films with continuously varied x. The sheet resistance of $Zn_{1-x}Mg_xO:Al$ film increased exponentially as the Mg content increased. To be an effective conductive window layer in CIGS solar cells, the resistivity must be around $1 \times 10^{-3} \Omega\text{-cm}$ or less. Thus, the electrical properties of the $Zn_{1-x}Mg_xO:Al$ film would only be acceptable when $x < 0.035$. More than 3.5 at% Mg would cause the film resistivity to be higher than $1 \times 10^{-3} \Omega\text{-cm}$.

Due to the doping effect, the optical bandgap could be fit by two equations for regions I and II. For $x < 0.07$, the bandgap can be expressed as $E_o = E_g + \Delta E_{gBN} + \Delta E_{gBM} + 1.938x$, and for $x > 0.07$, the bandgap can be expressed as $E_o = +E_{g(ZnO)} + 1.938x$. At $x = 0.035$, the optical bandgap is smaller than $x = 0$ due to the reversed Burstein-Moss effect. Thus, our result indicates that alloying $ZnO:Al$ with MgO will not optimize the conductive window layer for CIGS solar cells. Future work should include conducting this experiment with an undoped ZnO target to see whether the optical bandgap follows the equation $E_o = +E_{g(ZnO)} + 1.938x$ when $x < 0.07$.

ACKNOWLEDGEMENTS

This work was supported by the U.S. Department of Energy under Contract No. DE-AC36-99GO10337.

REFERENCES

1. D. Schmid, M. Ruckh, and H.W. Schock, *Solar Energy Materials and Solar Cells* **41/42**, 281, (1996).
2. S. Choopun, R.D. Vispute, W. Yang, R. P. Sharma, and T. Venkatesan, “Realization of band gap above 5.0 eV in metastable cubic-phase $Mg_xZn_{1-x}O$ films,” *Appl. Phys. Lett.* **80**, 1529, (2002).
3. K. Matsubara, H. Tampo, H. Shibata, A. Yamada, P. Fons, K. Iwata, and S. Niki, “Band-gap modified Al-doped $Zn_{1-x}Mg_xO$ transparent conducting films deposited by pulsed laser deposition,” *Applied Physics Letters* **85**, pp.1374–1376, 2004.
4. X. Li, D.L. Young, H. Moutinho, Y. Yan, C. Narayanswamy, T.A. Gessert, and T.J. Coutts, “Properties of CdO thin films produced by chemical vapor deposition,” *Electrochemical and Solid-State Letters* **4**, pp. C43–C46, 2001.
5. A. Ohtomo, M. Kawasaki, T. Koida, K. Masubuchi, H. Koinuma, Y. Sakurai, Y. Yoshida, T. Tasuda, and Y. Segawa, *Appl. Phys. Lett.* **72**, 2466, (1998).
6. T. Minemoto, T. Negami, S. Nishiwaki, H. Takakura, Y. hamakawa, *Thin Solid Films*, **372**, 173, (2000).
7. Sheng S. Li, *Semiconductor Physical Electronics*, 1993, Plenum Press, New York and London, ISBN 0-306-44157-8.
8. W.S. Baer, *Physical Review* **154**, 785, (1967).
9. E. Burstein, *Phys. Rev.* **93**, 632, (1954).
10. T.S. Moss, *Proc. Phys. Soc.* **B67**, 775 (1954).
11. V. Palankovski, G. Kaiblinger-Grujin, and S. Selberherr, *Materials Science and Engineering* **B66** 46, (1999).